



CERN-PH-EP-2013-128

LHCb-PAPER-2013-046

July 18, 2013

Measurement of the $B_s^0 \rightarrow \mu^+ \mu^-$ branching fraction and search for $B^0 \rightarrow \mu^+ \mu^-$ decays at the LHCb experiment

The LHCb collaboration¹

Abstract

A search for the rare decays $B_s^0 \rightarrow \mu^+ \mu^-$ and $B^0 \rightarrow \mu^+ \mu^-$ is performed at the LHCb experiment. The data analysed correspond to an integrated luminosity of 1 fb^{-1} of pp collisions at a centre-of-mass energy of 7 TeV and 2 fb^{-1} at 8 TeV. An excess of $B_s^0 \rightarrow \mu^+ \mu^-$ signal candidates with respect to the background expectation is seen with a significance of 4.0 standard deviations. A time-integrated branching fraction of $\mathcal{B}(B_s^0 \rightarrow \mu^+ \mu^-) = (2.9^{+1.1}_{-1.0}) \times 10^{-9}$ is obtained and an upper limit of $\mathcal{B}(B^0 \rightarrow \mu^+ \mu^-) < 7.4 \times 10^{-10}$ at 95% confidence level is set. These results are consistent with the Standard Model expectations.

Published in Phys. Rev. Lett. 111, 101805 (2013)

© CERN on behalf of the LHCb collaboration, license CC-BY-3.0.

¹Authors are listed on the following pages.

LHCb collaboration

R. Aaij⁴⁰, B. Adeva³⁶, M. Adinolfi⁴⁵, C. Adrover⁶, A. Affolder⁵¹, Z. Ajaltouni⁵, J. Albrecht⁹, F. Alessio³⁷, M. Alexander⁵⁰, S. Ali⁴⁰, G. Alkhazov²⁹, P. Alvarez Cartelle³⁶, A.A. Alves Jr^{24,37}, S. Amato², S. Amerio²¹, Y. Amhis⁷, L. Anderlini^{17,f}, J. Anderson³⁹, R. Andreassen⁵⁶, J.E. Andrews⁵⁷, R.B. Appleby⁵³, O. Aquines Gutierrez¹⁰, F. Archilli¹⁸, A. Artamonov³⁴, M. Artuso⁵⁸, E. Aslanides⁶, G. Auriemma^{24,m}, M. Baalouch⁵, S. Bachmann¹¹, J.J. Back⁴⁷, A. Badalov³⁵, C. Baesso⁵⁹, V. Balagura³⁰, W. Baldini¹⁶, R.J. Barlow⁵³, C. Barschel³⁷, S. Barsuk⁷, W. Barter⁴⁶, Th. Bauer⁴⁰, A. Bay³⁸, J. Beddow⁵⁰, F. Bedeschi²², I. Bediaga¹, S. Belogurov³⁰, K. Belous³⁴, I. Belyaev³⁰, E. Ben-Haim⁸, G. Bencivenni¹⁸, S. Benson⁴⁹, J. Benton⁴⁵, A. Berezhnoy³¹, R. Bernet³⁹, M.-O. Bettler⁴⁶, M. van Beuzekom⁴⁰, A. Bien¹¹, S. Bifani⁴⁴, T. Bird⁵³, A. Bizzeti^{17,h}, P.M. Björnstad⁵³, T. Blake³⁷, F. Blanc³⁸, S. Blusk⁵⁸, V. Bocci²⁴, A. Bondar³³, N. Bondar²⁹, W. Bonivento¹⁵, S. Borghi⁵³, A. Borgia⁵⁸, T.J.V. Bowcock⁵¹, E. Bowen³⁹, C. Bozzi¹⁶, T. Brambach⁹, J. van den Brand⁴¹, J. Bressieux³⁸, D. Brett⁵³, M. Britsch¹⁰, T. Britton⁵⁸, N.H. Brook⁴⁵, H. Brown⁵¹, I. Burducea²⁸, A. Bursche³⁹, G. Busetto^{21,q}, J. Buytaert³⁷, S. Cadeddu¹⁵, O. Callot⁷, M. Calvi^{20,j}, M. Calvo Gomez^{35,n}, A. Camboni³⁵, P. Campana^{18,37}, D. Campora Perez³⁷, A. Carbone^{14,c}, G. Carboni^{23,k}, R. Cardinale^{19,i}, A. Cardini¹⁵, H. Carranza-Mejia⁴⁹, L. Carson⁵², K. Carvalho Akiba², G. Casse⁵¹, L. Castillo Garcia³⁷, M. Cattaneo³⁷, Ch. Cauet⁹, R. Cenci⁵⁷, M. Charles⁵⁴, Ph. Charpentier³⁷, P. Chen^{3,38}, N. Chiapolini³⁹, M. Chrzaszcz^{39,25}, K. Ciba^{26,37}, X. Cid Vidal³⁷, G. Ciezarek⁵², P.E.L. Clarke⁴⁹, M. Clemencic³⁷, H.V. Cliff⁴⁶, J. Closier³⁷, C. Coca²⁸, V. Coco⁴⁰, J. Cogan⁶, E. Cogneras⁵, P. Collins³⁷, A. Comerma-Montells³⁵, A. Contu^{15,37}, A. Cook⁴⁵, M. Coombes⁴⁵, S. Coquereau⁸, G. Corti³⁷, B. Couturier³⁷, G.A. Cowan⁴⁹, E. Cowie⁴⁵, D.C. Craik⁴⁷, S. Cunliffe⁵², R. Currie⁴⁹, C. D'Ambrosio³⁷, P. David⁸, P.N.Y. David⁴⁰, A. Davis⁵⁶, I. De Bonis⁴, K. De Bruyn⁴⁰, S. De Capua⁵³, M. De Cian¹¹, J.M. De Miranda¹, L. De Paula², W. De Silva⁵⁶, P. De Simone¹⁸, D. Decamp⁴, M. Deckenhoff⁹, L. Del Buono⁸, N. Déleage⁴, D. Derkach⁵⁴, O. Deschamps⁵, F. Dettori⁴¹, A. Di Canto¹¹, H. Dijkstra³⁷, M. Dogaru²⁸, S. Donleavy⁵¹, F. Dordei¹¹, A. Dosil Suárez³⁶, D. Dossett⁴⁷, A. Dovbnya⁴², F. Dupertuis³⁸, P. Durante³⁷, R. Dzhelyadin³⁴, A. Dziurda²⁵, A. Dzyuba²⁹, S. Easo⁴⁸, U. Egede⁵², V. Egorychev³⁰, S. Eidelman³³, D. van Eijk⁴⁰, S. Eisenhardt⁴⁹, U. Eitschberger⁹, R. Ekelhof⁹, L. Eklund^{50,37}, I. El Rifai⁵, Ch. Elsasser³⁹, A. Falabella^{14,e}, C. Färber¹¹, C. Farinelli⁴⁰, S. Farry⁵¹, D. Ferguson⁴⁹, V. Fernandez Albor³⁶, F. Ferreira Rodrigues¹, M. Ferro-Luzzi³⁷, S. Filippov³², M. Fiore¹⁶, C. Fitzpatrick³⁷, M. Fontana¹⁰, F. Fontanelli^{19,i}, R. Forty³⁷, O. Francisco², M. Frank³⁷, C. Frei³⁷, M. Frosini^{17,37,f}, E. Furfaro^{23,k}, A. Gallas Torreira³⁶, D. Galli^{14,c}, M. Gandelman², P. Gandini⁵⁸, Y. Gao³, J. Garofoli⁵⁸, P. Garosi⁵³, J. Garra Tico⁴⁶, L. Garrido³⁵, C. Gaspar³⁷, R. Gauld⁵⁴, E. Gersabeck¹¹, M. Gersabeck⁵³, T. Gershon⁴⁷, Ph. Ghez⁴, V. Gibson⁴⁶, L. Giubega²⁸, V.V. Gligorov³⁷, C. Göbel⁵⁹, D. Golubkov³⁰, A. Golutvin^{52,30,37}, A. Gomes², P. Gorbounov^{30,37}, H. Gordon³⁷, C. Gotti²⁰, M. Grabalosa Gándara⁵, R. Graciani Diaz³⁵, L.A. Granado Cardoso³⁷, E. Graugés³⁵, G. Graziani¹⁷, A. Grecu²⁸, E. Greening⁵⁴, S. Gregson⁴⁶, P. Griffith⁴⁴, O. Grünberg⁶⁰, B. Gui⁵⁸, E. Gushchin³², Yu. Guz^{34,37}, T. Gys³⁷, C. Hadjivasiliou⁵⁸, G. Haefeli³⁸, C. Haen³⁷, S.C. Haines⁴⁶, S. Hall⁵², B. Hamilton⁵⁷, T. Hampson⁴⁵, S. Hansmann-Menzemer¹¹, N. Harnew⁵⁴, S.T. Harnew⁴⁵, J. Harrison⁵³, T. Hartmann⁶⁰, J. He³⁷, T. Head³⁷, V. Heijne⁴⁰, K. Hennessy⁵¹, P. Henrard⁵, J.A. Hernando Morata³⁶, E. van Herwijnen³⁷, M. Hess⁶⁰, A. Hicheur¹, E. Hicks⁵¹, D. Hill⁵⁴, M. Hoballah⁵, M. Holtrop⁴⁰, C. Hombach⁵³, W. Hulsbergen⁴⁰, P. Hunt⁵⁴, T. Huse⁵¹, N. Hussain⁵⁴, D. Hutchcroft⁵¹, D. Hynds⁵⁰, V. Iakovenko⁴³, M. Idzik²⁶, P. Ilten¹², R. Jacobsson³⁷, A. Jaeger¹¹, E. Jans⁴⁰, P. Jaton³⁸, A. Jawahery⁵⁷, F. Jing³, M. John⁵⁴, D. Johnson⁵⁴, C.R. Jones⁴⁶, C. Joram³⁷, B. Jost³⁷, M. Kabbalo⁹, S. Kandybei⁴², W. Kanso⁶, M. Karacson³⁷, T.M. Karbach³⁷, I.R. Kenyon⁴⁴, T. Ketel⁴¹, B. Khanji²⁰, O. Kochebina⁷, I. Komarov³⁸, R.F. Koopman⁴¹, P. Koppenburg⁴⁰, M. Korolev³¹, A. Kozlinskiy⁴⁰, L. Kravchuk³², K. Kreplin¹¹, M. Kreps⁴⁷, G. Krocker¹¹, P. Krokovny³³, F. Kruse⁹, M. Kucharczyk^{20,25,37,j}, V. Kudryavtsev³³, K. Kurek²⁷, T. Kvaratskheliya^{30,37}, V.N. La Thi³⁸, D. Lacarrere³⁷, G. Lafferty⁵³, A. Lai¹⁵, D. Lambert⁴⁹, R.W. Lambert⁴¹, E. Lanciotti³⁷, G. Lanfranchi¹⁸, C. Langenbruch³⁷, T. Latham⁴⁷, C. Lazzeroni⁴⁴, R. Le Gac⁶, J. van Leerdam⁴⁰, J.-P. Lees⁴, R. Lefèvre⁵, A. Leflat³¹, J. Lefrançois⁷, S. Leo²², O. Leroy⁶, T. Lesiak²⁵, B. Leverington¹¹, Y. Li³, L. Li Gioi⁵, M. Liles⁵¹, R. Lindner³⁷, C. Linn¹¹, B. Liu³, G. Liu³⁷, S. Lohm³⁷, I. Longstaff⁵⁰, J.H. Lopes², N. Lopez-March³⁸, H. Lu³, D. Lucchesi^{21,q}, J. Luisier³⁸, H. Luo⁴⁹, F. Machefert⁷, I.V. Machikhiliyan^{4,30}, F. Maciuc²⁸, O. Maev^{29,37}, S. Malde⁵⁴, G. Manca^{15,d}, G. Mancinelli⁶, J. Maratas⁵, U. Marconi¹⁴, P. Marino^{22,s}, R. Märki³⁸, J. Marks¹¹, G. Martellotti²⁴, A. Martens⁸, A. Martín Sánchez⁷, M. Martinelli⁴⁰, D. Martinez Santos^{41,37}, D. Martins Tostes², A. Martynov³¹, A. Massafferri¹, R. Matev³⁷, Z. Mathe³⁷, C. Matteuzzi²⁰, E. Maurice⁶, A. Mazurov^{16,32,37,e}, J. McCarthy⁴⁴, A. McNab⁵³, R. McNulty¹², B. McKelley⁵¹, B. Meadows^{56,54}, F. Meier⁹, M. Meissner¹¹, M. Merk⁴⁰, D.A. Milanes⁸, M.-N. Minard⁴, J. Molina Rodriguez⁵⁹, S. Monteil⁵, D. Moran⁵³, P. Morawski²⁵, A. Mordà⁶, M.J. Morello^{22,s}, R. Mountain⁵⁸, I. Mous⁴⁰, F. Muheim⁴⁹, K. Müller³⁹, R. Muresan²⁸, B. Muryn²⁶, B. Muster³⁸, P. Naik⁴⁵, T. Nakada³⁸, R. Nandakumar⁴⁸, I. Nasteva¹, M. Needham⁴⁹, S. Neubert³⁷, N. Neufeld³⁷, A.D. Nguyen³⁸, T.D. Nguyen³⁸, C. Nguyen-Mau^{38,o}, M. Nicol⁷, V. Niess⁵, R. Niet⁹, N. Nikitin³¹, T. Nikodem¹¹, A. Nomerotski⁵⁴, A. Novoselov³⁴, A. Oblakowska-Mucha²⁶, V. Obraztsov³⁴, S. Oggero⁴⁰, S. Ogilvy⁵⁰, O. Okhrimenko⁴³, R. Oldeman^{15,d}, M. Orlandea²⁸, J.M. Otarola Goicochea², P. Owen⁵², A. Oyanguren³⁵, B.K. Pal⁵⁸, A. Palano^{13,b}, T. Palczewski²⁷, M. Palutan¹⁸, J. Panman³⁷, A. Papanestis⁴⁸, M. Pappagallo⁵⁰, C. Parkes⁵³, C.J. Parkinson⁵², G. Passaleva¹⁷, G.D. Patel⁵¹, M. Patel⁵², G.N. Patrick⁴⁸, C. Patrignani^{19,i}, C. Pavel-Nicorescu²⁸, A. Pazos Alvarez³⁶, A. Pellegrino⁴⁰, G. Penso^{24,l}, M. Pepe Altarelli³⁷, S. Perazzini^{14,c}, E. Perez Trigo³⁶, A. Pérez-Calero Yzquierdo³⁵, P. Perret⁵, M. Perrin-Terrin⁶,

L. Pescatore⁴⁴, E. Pesen⁶¹, K. Petridis⁵², A. Petrolini^{19,i}, A. Phan⁵⁸, E. Picatoste Olloqui³⁵, B. Pietrzyk⁴, T. Pilar⁴⁷, D. Pinci²⁴, S. Playfer⁴⁹, M. Plo Casasus³⁶, F. Polci⁸, G. Polok²⁵, A. Poluektov^{47,33}, E. Polycarpo², A. Popov³⁴, D. Popov¹⁰, B. Popovici²⁸, C. Potterat³⁵, A. Powell⁵⁴, J. Prisciandaro³⁸, A. Pritchard⁵¹, C. Prouve⁷, V. Pugatch⁴³, A. Puig Navarro³⁸, G. Punzi^{22,r}, W. Qian⁴, J.H. Rademacker⁴⁵, B. Rakotomiamanana³⁸, M.S. Rangel², I. Raniuk⁴², N. Rauschmayr³⁷, G. Raven⁴¹, S. Redford⁵⁴, S. Reichert⁵³, M.M. Reid⁴⁷, A.C. dos Reis¹, S. Ricciardi⁴⁸, A. Richards⁵², K. Rinnert⁵¹, V. Rives Molina³⁵, D.A. Roa Romero⁵, P. Robbe⁷, D.A. Roberts⁵⁷, E. Rodrigues⁵³, P. Rodriguez Perez³⁶, S. Roiser³⁷, V. Romanovsky³⁴, A. Romero Vidal³⁶, J. Rouvinet³⁸, T. Ruf³⁷, F. Ruffini²², H. Ruiz³⁵, P. Ruiz Valls³⁵, G. Sabatino^{24,k}, J.J. Saborido Silva³⁶, N. Sagidova²⁹, P. Sail⁵⁰, B. Saitta^{15,d}, V. Salustino Guimaraes², B. Sanmartin Sedes³⁶, R. Santacesaria²⁴, C. Santamarina Rios³⁶, E. Santovetti^{23,k}, M. Sapunov⁶, A. Sarti^{18,l}, C. Satriano^{24,m}, A. Satta²³, M. Savrie^{16,e}, D. Savrina^{30,31}, M. Schiller⁴¹, H. Schindler³⁷, M. Schlupp⁹, M. Schmelling¹⁰, B. Schmidt³⁷, O. Schneider³⁸, A. Schopper³⁷, M.-H. Schune⁷, R. Schwemmer³⁷, B. Sciascia¹⁸, A. Sciubba²⁴, M. Seco³⁶, A. Semennikov³⁰, K. Senderowska²⁶, I. Sepp⁵², N. Serra³⁹, J. Serrano⁶, P. Seyfert¹¹, M. Shapkin³⁴, I. Shapoval^{16,42}, P. Shatalov³⁰, Y. Shcheglov²⁹, T. Shears⁵¹, L. Shekhtman³³, O. Shevchenko⁴², V. Shevchenko³⁰, A. Shires⁹, R. Silva Coutinho⁴⁷, M. Sirendi⁴⁶, N. Skidmore⁴⁵, T. Skwarnicki⁵⁸, N.A. Smith⁵¹, E. Smith^{54,48}, J. Smith⁴⁶, M. Smith⁵³, M.D. Sokoloff⁵⁶, F.J.P. Soler⁵⁰, F. Soomro³⁸, D. Souza⁴⁵, B. Souza De Paula², B. Spaan⁹, A. Sparkes⁴⁹, P. Spradlin⁵⁰, F. Stagni³⁷, S. Stahl¹¹, O. Steinkamp³⁹, S. Stevenson⁵⁴, S. Stoica²⁸, S. Stone⁵⁸, B. Storaci³⁹, M. Straticiuc²⁸, U. Straumann³⁹, V.K. Subbiah³⁷, L. Sun⁵⁶, S. Swientek⁹, V. Syropoulos⁴¹, M. Szczekowski²⁷, P. Szczypka^{38,37}, T. Szumlak²⁶, S. T'Jampens⁴, M. Teklishyn⁷, E. Teodorescu²⁸, F. Teubert³⁷, C. Thomas⁵⁴, E. Thomas³⁷, J. van Tilburg¹¹, V. Tisserand⁴, M. Tobin³⁸, S. Tolk⁴¹, D. Tonelli³⁷, S. Topp-Joergensen⁵⁴, N. Torr⁵⁴, E. Tournefier^{4,52}, S. Tourneur³⁸, M.T. Tran³⁸, M. Tresch³⁹, A. Tsaregorodtsev⁶, P. Tsopelas⁴⁰, N. Tuning^{40,37}, M. Ubeda Garcia³⁷, A. Ukleja²⁷, A. Ustyuzhanin^{52,p}, U. Uwer¹¹, V. Vagnoni¹⁴, G. Valentini¹⁴, A. Vallier⁷, M. Van Dijk⁴⁵, R. Vazquez Gomez¹⁸, P. Vazquez Regueiro³⁶, C. Vázquez Sierra³⁶, S. Vecchi¹⁶, J.J. Velthuis⁴⁵, M. Veltri^{17,9}, G. Veneziano³⁸, M. Vesterinen³⁷, B. Viaud⁷, D. Vieira², X. Vilasis-Cardona^{35,n}, A. Vollhardt³⁹, D. Volyanskyy¹⁰, D. Voong⁴⁵, A. Vorobyev²⁹, V. Vorobyev³³, C. Voz⁶⁰, H. Voss¹⁰, R. Waldi⁶⁰, C. Wallace⁴⁷, R. Wallace¹², S. Wandernoth¹¹, J. Wang⁵⁸, D.R. Ward⁴⁶, N.K. Watson⁴⁴, A.D. Webber⁵³, D. Websdale⁵², M. Whitehead⁴⁷, J. Wicht³⁷, J. Wiechczynski²⁵, D. Wiedner¹¹, L. Wiggers⁴⁰, G. Wilkinson⁵⁴, M.P. Williams^{47,48}, M. Williams⁵⁵, F.F. Wilson⁴⁸, J. Wimberley⁵⁷, J. Wishahi⁹, W. Wislicki²⁷, M. Witek²⁵, G. Wormser⁷, S.A. Wotton⁴⁶, S. Wright⁴⁶, S. Wu³, K. Wyllie³⁷, Y. Xie^{49,37}, Z. Xing⁵⁸, Z. Yang³, X. Yuan³, O. Yushchenko³⁴, M. Zangoli¹⁴, M. Zavertyaev^{10,a}, F. Zhang³, L. Zhang⁵⁸, W.C. Zhang¹², Y. Zhang³, A. Zhelezov¹¹, A. Zhokhov³⁰, L. Zhong³, A. Zvyagin³⁷.

¹ Centro Brasileiro de Pesquisas Físicas (CBPF), Rio de Janeiro, Brazil

² Universidade Federal do Rio de Janeiro (UFRJ), Rio de Janeiro, Brazil

³ Center for High Energy Physics, Tsinghua University, Beijing, China

⁴ LAPP, Université de Savoie, CNRS/IN2P3, Annecy-Le-Vieux, France

⁵ Clermont Université, Université Blaise Pascal, CNRS/IN2P3, LPC, Clermont-Ferrand, France

⁶ CPPM, Aix-Marseille Université, CNRS/IN2P3, Marseille, France

⁷ LAL, Université Paris-Sud, CNRS/IN2P3, Orsay, France

⁸ LPNHE, Université Pierre et Marie Curie, Université Paris Diderot, CNRS/IN2P3, Paris, France

⁹ Fakultät Physik, Technische Universität Dortmund, Dortmund, Germany

¹⁰ Max-Planck-Institut für Kernphysik (MPIK), Heidelberg, Germany

¹¹ Physikalisches Institut, Ruprecht-Karls-Universität Heidelberg, Heidelberg, Germany

¹² School of Physics, University College Dublin, Dublin, Ireland

¹³ Sezione INFN di Bari, Bari, Italy

¹⁴ Sezione INFN di Bologna, Bologna, Italy

¹⁵ Sezione INFN di Cagliari, Cagliari, Italy

¹⁶ Sezione INFN di Ferrara, Ferrara, Italy

¹⁷ Sezione INFN di Firenze, Firenze, Italy

¹⁸ Laboratori Nazionali dell'INFN di Frascati, Frascati, Italy

¹⁹ Sezione INFN di Genova, Genova, Italy

²⁰ Sezione INFN di Milano Bicocca, Milano, Italy

²¹ Sezione INFN di Padova, Padova, Italy

²² Sezione INFN di Pisa, Pisa, Italy

²³ Sezione INFN di Roma Tor Vergata, Roma, Italy

²⁴ Sezione INFN di Roma La Sapienza, Roma, Italy

²⁵ Henryk Niewodniczanski Institute of Nuclear Physics Polish Academy of Sciences, Kraków, Poland

²⁶ AGH - University of Science and Technology, Faculty of Physics and Applied Computer Science, Kraków, Poland

²⁷ National Center for Nuclear Research (NCBJ), Warsaw, Poland

²⁸ Horia Hulubei National Institute of Physics and Nuclear Engineering, Bucharest-Magurele, Romania

²⁹ Petersburg Nuclear Physics Institute (PNPI), Gatchina, Russia

³⁰ Institute of Theoretical and Experimental Physics (ITEP), Moscow, Russia

³¹ Institute of Nuclear Physics, Moscow State University (SINP MSU), Moscow, Russia

³² Institute for Nuclear Research of the Russian Academy of Sciences (INR RAN), Moscow, Russia

- ³³ *Budker Institute of Nuclear Physics (SB RAS) and Novosibirsk State University, Novosibirsk, Russia*
- ³⁴ *Institute for High Energy Physics (IHEP), Protvino, Russia*
- ³⁵ *Universitat de Barcelona, Barcelona, Spain*
- ³⁶ *Universidad de Santiago de Compostela, Santiago de Compostela, Spain*
- ³⁷ *European Organization for Nuclear Research (CERN), Geneva, Switzerland*
- ³⁸ *Ecole Polytechnique Fédérale de Lausanne (EPFL), Lausanne, Switzerland*
- ³⁹ *Physik-Institut, Universität Zürich, Zürich, Switzerland*
- ⁴⁰ *Nikhef National Institute for Subatomic Physics, Amsterdam, The Netherlands*
- ⁴¹ *Nikhef National Institute for Subatomic Physics and VU University Amsterdam, Amsterdam, The Netherlands*
- ⁴² *NSC Kharkiv Institute of Physics and Technology (NSC KIPT), Kharkiv, Ukraine*
- ⁴³ *Institute for Nuclear Research of the National Academy of Sciences (KINR), Kyiv, Ukraine*
- ⁴⁴ *University of Birmingham, Birmingham, United Kingdom*
- ⁴⁵ *H.H. Wills Physics Laboratory, University of Bristol, Bristol, United Kingdom*
- ⁴⁶ *Cavendish Laboratory, University of Cambridge, Cambridge, United Kingdom*
- ⁴⁷ *Department of Physics, University of Warwick, Coventry, United Kingdom*
- ⁴⁸ *STFC Rutherford Appleton Laboratory, Didcot, United Kingdom*
- ⁴⁹ *School of Physics and Astronomy, University of Edinburgh, Edinburgh, United Kingdom*
- ⁵⁰ *School of Physics and Astronomy, University of Glasgow, Glasgow, United Kingdom*
- ⁵¹ *Oliver Lodge Laboratory, University of Liverpool, Liverpool, United Kingdom*
- ⁵² *Imperial College London, London, United Kingdom*
- ⁵³ *School of Physics and Astronomy, University of Manchester, Manchester, United Kingdom*
- ⁵⁴ *Department of Physics, University of Oxford, Oxford, United Kingdom*
- ⁵⁵ *Massachusetts Institute of Technology, Cambridge, MA, United States*
- ⁵⁶ *University of Cincinnati, Cincinnati, OH, United States*
- ⁵⁷ *University of Maryland, College Park, MD, United States*
- ⁵⁸ *Syracuse University, Syracuse, NY, United States*
- ⁵⁹ *Pontificia Universidade Católica do Rio de Janeiro (PUC-Rio), Rio de Janeiro, Brazil, associated to ²*
- ⁶⁰ *Institut für Physik, Universität Rostock, Rostock, Germany, associated to ¹¹*
- ⁶¹ *Celal Bayar University, Manisa, Turkey, associated to ³⁷*

^a *P.N. Lebedev Physical Institute, Russian Academy of Science (LPI RAS), Moscow, Russia*

^b *Università di Bari, Bari, Italy*

^c *Università di Bologna, Bologna, Italy*

^d *Università di Cagliari, Cagliari, Italy*

^e *Università di Ferrara, Ferrara, Italy*

^f *Università di Firenze, Firenze, Italy*

^g *Università di Urbino, Urbino, Italy*

^h *Università di Modena e Reggio Emilia, Modena, Italy*

ⁱ *Università di Genova, Genova, Italy*

^j *Università di Milano Bicocca, Milano, Italy*

^k *Università di Roma Tor Vergata, Roma, Italy*

^l *Università di Roma La Sapienza, Roma, Italy*

^m *Università della Basilicata, Potenza, Italy*

ⁿ *LIFAELS, La Salle, Universitat Ramon Llull, Barcelona, Spain*

^o *Hanoi University of Science, Hanoi, Viet Nam*

^p *Institute of Physics and Technology, Moscow, Russia*

^q *Università di Padova, Padova, Italy*

^r *Università di Pisa, Pisa, Italy*

^s *Scuola Normale Superiore, Pisa, Italy*

The rare decays $B_s^0 \rightarrow \mu^+\mu^-$ and $B^0 \rightarrow \mu^+\mu^-$ are highly suppressed and their branching fractions precisely predicted in the standard model (SM); any observed deviation would therefore be a clear sign of physics beyond the SM, for example a nonstandard Higgs sector. The SM predicts branching fractions of $\mathcal{B}(B_s^0 \rightarrow \mu^+\mu^-) = (3.35 \pm 0.28) \times 10^{-9}$ and $\mathcal{B}(B^0 \rightarrow \mu^+\mu^-) = (1.07 \pm 0.10) \times 10^{-10}$. These theoretical predictions are for decays at decay time $t = 0$, and have been updated with respect to Refs. [1, 2] using the latest average for the B_s^0 meson lifetime, $\tau_{B_s^0} = 1.516 \pm 0.011$ ps [3]. The uncertainty is dominated by the precision of lattice QCD calculations of the decay constants [1, 4–7]. In the B_s^0 system, due to the finite width difference, the comparison between the above prediction and the measured time-integrated branching fraction requires a model-dependent correction [8]. The SM time-integrated prediction is therefore $\mathcal{B}(B_s^0 \rightarrow \mu^+\mu^-) = (3.56 \pm 0.30) \times 10^{-9}$, using the relative decay width difference $\Delta\Gamma_s/(2\Gamma_s) = 0.0615 \pm 0.0085$ [3].

The first search for dimuon decays of B mesons took place 30 years ago [9]. Since then, possible deviations from the SM prediction have been constrained by various searches, with the most recent results available in Refs. [10–14]. The first evidence for the $B_s^0 \rightarrow \mu^+\mu^-$ decay was reported by LHCb in Ref. [12], with $\mathcal{B}(B_s^0 \rightarrow \mu^+\mu^-) = (3.2_{-1.2}^{+1.5}) \times 10^{-9}$, together with the lowest limit on the B^0 decay, $\mathcal{B}(B^0 \rightarrow \mu^+\mu^-) < 9.4 \times 10^{-10}$ at 95% confidence level (CL). The results presented in this Letter improve on and supersede our previous measurements [12]. They are based on data collected with the LHCb detector, corresponding to an integrated luminosity of 1 fb^{-1} of pp collisions at the LHC recorded in 2011 at a centre-of-mass energy $\sqrt{s} = 7 \text{ TeV}$, and 2 fb^{-1} recorded in 2012 at $\sqrt{s} = 8 \text{ TeV}$. These data include an additional 1 fb^{-1} compared to the sample analysed in Ref. [12], and have been reconstructed with improved algorithms and detector alignment parameters leading to slightly higher signal reconstruction efficiency and better invariant mass resolution. The samples from the two centre-of-mass energies are analysed as a combined dataset.

The analysis strategy is very similar to that employed in Ref. [12], with a different multivariate operator based on a boosted decision trees algorithm (BDT) [15, 16]. After trigger and loose selection requirements, $B_{(s)}^0 \rightarrow \mu^+\mu^-$ candidates are classified according to dimuon invariant mass and BDT output. The distribution of candidates is compared with the background estimates to determine the signal yield and significance. The signal yield is converted into a

branching fraction using a relative normalisation to the channels $B^0 \rightarrow K^+\pi^-$ and $B^+ \rightarrow J/\psi K^+$ with $J/\psi \rightarrow \mu^+\mu^-$. Inclusion of charge-conjugated processes is implied throughout this Letter. To avoid potential biases, candidates in the signal regions were not examined until the analysis procedure had been finalised.

The LHCb detector is a single-arm forward spectrometer covering the pseudorapidity range $2 < \eta < 5$, described in detail in Ref. [17]. The simulated events used in this analysis are produced using the software described in Refs. [18–23].

Signal and normalisation candidate events are selected by a hardware trigger and a subsequent software trigger [24]. The $B_{(s)}^0 \rightarrow \mu^+\mu^-$ candidates are predominantly selected by single-muon and dimuon triggers. Candidate $B^+ \rightarrow J/\psi K^+$ decays are selected in a similar way, the only difference being a different dimuon mass requirement in the software trigger. Candidate $B_{(s)}^0 \rightarrow h^+h'^-$ decays (where $h^{(\prime)} = \pi, K$), used as control channels, are required to be triggered independently of the $B_{(s)}^0$ decay products.

Candidate $B_{(s)}^0 \rightarrow \mu^+\mu^-$ decays are selected by combining two oppositely charged tracks with high quality muon identification [25], transverse momentum p_T satisfying $0.25 < p_T < 40 \text{ GeV}/c$, and momentum $p < 500 \text{ GeV}/c$. The two tracks are required to form a secondary vertex (SV), with χ^2 per degree of freedom less than 9, displaced from any pp interaction vertex (primary vertex, PV) by a flight distance significance greater than 15. The smallest impact parameter χ^2 (χ_{IP}^2), defined as the difference between the χ^2 of a PV formed with and without the track in question, is required to be larger than 25 with respect to any PV for the muon candidates. Only B candidates with $p_T > 0.5 \text{ GeV}/c$, decay time less than $9 \times \tau_{B_s^0}$ [3], impact parameter significance $\text{IP}/\sigma(\text{IP}) < 5$ with respect to the PV for which the B IP is minimal, and dimuon invariant mass in the range $[4900, 6000] \text{ MeV}/c^2$ are selected. The control and normalisation channels are selected with almost identical requirements to those applied to the signal sample. The $B_{(s)}^0 \rightarrow h^+h'^-$ selection is the same as that of $B_{(s)}^0 \rightarrow \mu^+\mu^-$, except that muon identification criteria are not applied. The $B^+ \rightarrow J/\psi K^+$ decay is reconstructed from a dimuon pair combined to form the $J/\psi \rightarrow \mu^+\mu^-$ decay and selected in the same way as the $B_{(s)}^0 \rightarrow \mu^+\mu^-$ signal samples, except for the requirements on the impact parameter significance and mass. After a requirement of $\chi_{\text{IP}}^2 > 25$, kaon candidates are combined with the J/ψ candidates. These selection criteria are completed by

a requirement on the response of a multivariate operator, called MVS in Ref. [26] and unchanged since then, applied to candidates in both signal and normalisation channels. After the trigger and selection requirements are applied, 55 661 signal dimuon candidates are found, which are used for the search.

The main discrimination between the signal and combinatorial background is brought by the BDT, which is optimised using simulated samples of $B_s^0 \rightarrow \mu^+\mu^-$ events for the signal and $b\bar{b} \rightarrow \mu^+\mu^-X$ events for the background. The BDT combines information from the following input variables: the B candidate decay time, IP and p_T ; the minimum χ_{IP}^2 of the two muons with respect to any PV; the distance of closest approach between the two muons; and the cosine of the angle between the muon momentum in the dimuon rest frame and the vector perpendicular to both the B candidate momentum and the beam axis. Moreover two different measures for the isolation of signal candidates are also included: the number of good two-track vertices a muon can make with other tracks in the event; and the B candidate isolation, introduced in Ref. [27]. With respect to the multivariate operator used in previous analyses [12,26], the minimum p_T of the two muons is no longer used while four new variables are included to improve the separation power. The first two are the absolute values of the differences between the pseudorapidities of the two muon candidates and between their azimuthal angles. The others are the angle of the momentum of the B candidate in the laboratory frame, and the angle of the positive muon from the B candidate in the rest frame of the B candidate, both with respect to the sum of the momenta of tracks, in the rest frame of the B candidate, consistent with originating from the decay of a b hadron produced in association to the signal candidate. In total, 12 variables enter into the BDT.

The variables used in the BDT are chosen so that the dependence on dimuon invariant mass is linear and small to avoid biases. The BDT is constructed to be distributed uniformly in the range [0,1] for signal, and to peak strongly at zero for the background. The BDT response range is divided into eight bins with boundaries 0.0, 0.25, 0.4, 0.5, 0.6, 0.7, 0.8, 0.9, and 1.0.

The expected BDT distributions for the $B_{(s)}^0 \rightarrow \mu^+\mu^-$ signals are determined using $B_{(s)}^0 \rightarrow h^+h'^-$ decays. The $B_{(s)}^0 \rightarrow h^+h'^-$ distributions are corrected for trigger and muon identification distortions. An additional correction for the $B_s^0 \rightarrow \mu^+\mu^-$ signal arises from the difference in lifetime acceptance in BDT bins, evaluated assuming the SM decay time distribution.

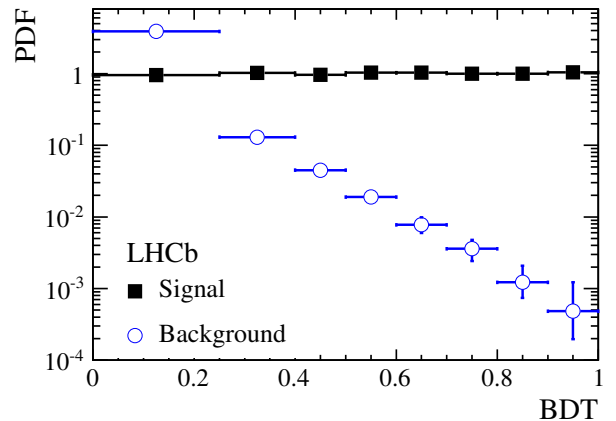


Figure 1: Expected distribution of the BDT output for the $B_s^0 \rightarrow \mu^+\mu^-$ signal (black squares), obtained from $B_{(s)}^0 \rightarrow h^+h'^-$ control channels, and the combinatorial background (blue circles).

The expected $B_s^0 \rightarrow \mu^+\mu^-$ BDT distribution is shown in Fig. 1.

The invariant mass distribution of the signal decays is described by a Crystal Ball function [28]. The peak values ($m_{B_s^0}$ and m_{B^0}) and resolutions ($\sigma_{B_s^0}$ and σ_{B^0}) are obtained from $B_s^0 \rightarrow K^+K^-$ and $B^0 \rightarrow K^+\pi^-$, $B^0 \rightarrow \pi^+\pi^-$ decays, for the B_s^0 and B^0 mesons. The resolutions are also determined with a power-law interpolation between the measured resolutions of charmonium and bottomonium resonances decaying into two muons. The two methods are in agreement and the combined results are $\sigma_{B_s^0} = 23.2 \pm 0.4 \text{ MeV}/c^2$ and $\sigma_{B^0} = 22.8 \pm 0.4 \text{ MeV}/c^2$. The transition point of the radiative tail is obtained from simulated $B_s^0 \rightarrow \mu^+\mu^-$ events [21] smeared to reproduce the mass resolution measured in data.

The numbers of $B_s^0 \rightarrow \mu^+\mu^-$ and $B^0 \rightarrow \mu^+\mu^-$ candidates, $N_{B_{(s)}^0 \rightarrow \mu^+\mu^-}$, are converted into branching fractions with

$$\begin{aligned} \mathcal{B}(B_{(s)}^0 \rightarrow \mu^+\mu^-) &= \frac{\mathcal{B}_{\text{norm}} \epsilon_{\text{norm}} f_{\text{norm}}}{N_{\text{norm}} \epsilon_{\text{sig}} f_{d(s)}} \times N_{B_{(s)}^0 \rightarrow \mu^+\mu^-} \\ &= \alpha_{B_{(s)}^0 \rightarrow \mu^+\mu^-}^{\text{norm}} \times N_{B_{(s)}^0 \rightarrow \mu^+\mu^-}, \end{aligned}$$

where N_{norm} is the number of normalisation channel decays obtained from a fit to the relevant invariant mass distribution, and $\mathcal{B}_{\text{norm}}$ the corresponding branching fraction. The fractions $f_{d(s)}$ and f_{norm} refer to the probability for a b quark to fragment into the corresponding B meson. The value $f_s/f_d = 0.259 \pm 0.015$, measured by LHCb in pp collision data at $\sqrt{s} = 7 \text{ TeV}$ [29,30],

is used and $f_d = f_u$ is assumed. The stability of f_s/f_u between $\sqrt{s} = 7$ TeV and 8 TeV is verified by comparing the ratios of the yields of $B_s^0 \rightarrow J/\psi\phi$ and $B^+ \rightarrow J/\psi K^+$ decays. The effect of the measured dependence of f_s/f_d on p_T [29] is found to be negligible.

The efficiency $\epsilon_{\text{sig(norm)}}$ for the signal (normalisation) channel is the product of the reconstruction efficiency of the final state particles including the geometric detector acceptance, the selection efficiency and the trigger efficiency. The ratio of acceptance, reconstruction and selection efficiencies of the signal compared to the normalisation channel is computed with samples of simulated events, assuming the SM decay time distribution, corrected to take into account known differences between data and simulation. The tracking and particle identification efficiencies are measured from control channels in data. Residual differences between data and simulation are treated as sources of systematic uncertainty. The trigger efficiency is evaluated with data-driven techniques [24].

The observed numbers of $B^+ \rightarrow J/\psi K^+$ and $B^0 \rightarrow K^+ \pi^-$ decays are $(1.1164 \pm 0.0011) \times 10^6$ and $(3.76 \pm 0.06) \times 10^4$, respectively. The normalisation factors $\alpha_{B_{(s)}^0 \rightarrow \mu^+ \mu^-}^{\text{norm}}$ derived from the two channels are consistent. Their weighted averages, taking correlations into account, are $\alpha_{B_s^0 \rightarrow \mu^+ \mu^-} = (9.01 \pm 0.62) \times 10^{-11}$ and $\alpha_{B^0 \rightarrow \mu^+ \mu^-} = (2.40 \pm 0.09) \times 10^{-11}$. Assuming the $B_{(s)}^0 \rightarrow \mu^+ \mu^-$ SM branching fractions, the selected data sample is therefore expected to contain 40 ± 4 $B_s^0 \rightarrow \mu^+ \mu^-$ and 4.5 ± 0.4 $B^0 \rightarrow \mu^+ \mu^-$ decays in the full BDT range and with mass in $[4900, 6000]$ MeV/ c^2 .

Invariant mass sidebands are defined as $[4900, m_{B^0} - 60]$ MeV/ c^2 and $[m_{B_s^0} + 60, 6000]$ MeV/ c^2 . The low-mass sideband and the B^0 and B_s^0 signal regions contain a small amount of background from

Table 1: Expected background yields from b -hadron decays, with dimuon mass $m_{\mu\mu} \in [4900, 6000]$ MeV/ c^2 and the relative fraction with BDT > 0.7 .

	Yield in full BDT range	Fraction with BDT > 0.7 [%]
$B_{(s)}^0 \rightarrow h^+ h'^-$	15 \pm 1	28
$B^0 \rightarrow \pi^- \mu^+ \nu_\mu$	115 \pm 6	15
$B_s^0 \rightarrow K^- \mu^+ \nu_\mu$	10 \pm 4	21
$B^{0(+)} \rightarrow \pi^{0(+)} \mu^+ \mu^-$	28 \pm 8	15
$\Lambda_b^0 \rightarrow p \mu^- \bar{\nu}_\mu$	70 \pm 30	11

specific b -hadron decays. A subset of this background requires the misidentification of one or both of the candidate muons and includes $B^0 \rightarrow \pi^- \mu^+ \nu_\mu$, $B_{(s)}^0 \rightarrow h^+ h'^-$, $B_s^0 \rightarrow K^- \mu^+ \nu_\mu$, and $\Lambda_b^0 \rightarrow p \mu^- \bar{\nu}_\mu$ decays. In order to estimate the contribution from these processes, the $B^0 \rightarrow \pi^- \mu^+ \nu_\mu$ and $B_{(s)}^0 \rightarrow h^+ h'^-$ branching fractions are taken from Ref. [31], while, in the absence of measurements, theoretical estimates of the $\Lambda_b^0 \rightarrow p \mu^- \bar{\nu}_\mu$ [32] and $B_s^0 \rightarrow K^- \mu^+ \nu_\mu$ [33] branching fractions are used. Misidentification probabilities for the tracks in these decays are measured directly with control channels in data. Background sources without any misidentification such as $B_c^+ \rightarrow J/\psi \mu^+ \nu_\mu$ [34] and $B^{0(+)} \rightarrow \pi^{0(+)} \mu^+ \mu^-$ [35] decays are also considered. The expected yields of all the b -hadron background modes are estimated by normalising to the $B^+ \rightarrow J/\psi K^+$ decay with the exception of $B_{(s)}^0 \rightarrow h^+ h'^-$, for which the explicit selection yields are used, correcting for the trigger efficiency ratio. No veto is imposed on photons, as the contribution of $B_s^0 \rightarrow \mu^+ \mu^- \gamma$ is negligible, as are contributions from $B_s^0 \rightarrow \mu^+ \mu^- \nu_\mu \bar{\nu}_\mu$ decays [36, 37]. The expected number of events for each of the backgrounds from b -hadron decays is shown in Table 1. The only one of these contributions that is relevant under the signal mass peaks is from $B_{(s)}^0 \rightarrow h^+ h'^-$ decays.

A simultaneous unbinned maximum-likelihood fit to the data is performed in the mass projections of the BDT bins to determine the $B_s^0 \rightarrow \mu^+ \mu^-$ and $B^0 \rightarrow \mu^+ \mu^-$ branching fractions, which are free parameters. The $B_s^0 \rightarrow \mu^+ \mu^-$ and $B^0 \rightarrow \mu^+ \mu^-$ fractional yields in BDT bins are constrained to the BDT fractions calibrated with the $B_{(s)}^0 \rightarrow h^+ h'^-$ sample. The parameters of the Crystal Ball functions, that describe the mass shapes, and the normalisation factors are restricted by Gaussian constraints according to their expected values and uncertainties. The backgrounds from $B_{(s)}^0 \rightarrow h^+ h'^-$, $B^0 \rightarrow \pi^- \mu^+ \nu_\mu$, $B_s^0 \rightarrow K^- \mu^+ \nu_\mu$ and $B^{0(+)} \rightarrow \pi^{0(+)} \mu^+ \mu^-$ are included as separate components in the fit. The fractional yields of the b -hadron backgrounds in each BDT bin and their overall yields are limited by Gaussian constraints around the expected values according to their uncertainties. The combinatorial background in each BDT bin is parametrised with an exponential function for which both the slope and the normalisation are allowed to vary freely. The resulting BDT distribution is compared to that expected for the signal in Fig. 1.

An excess of $B_s^0 \rightarrow \mu^+ \mu^-$ candidates with respect to the expectation from the background only is seen

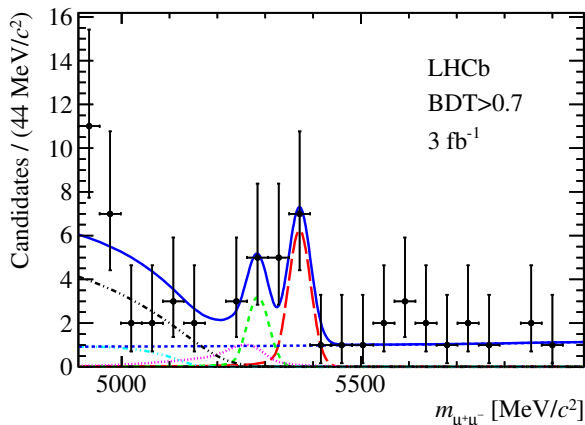


Figure 2: Invariant mass distribution of the selected $B_{(s)}^0 \rightarrow \mu^+\mu^-$ candidates (black dots) with $\text{BDT} > 0.7$. The result of the fit is overlaid (blue solid line) and the different components detailed: $B_s^0 \rightarrow \mu^+\mu^-$ (red long dashed line), $B^0 \rightarrow \mu^+\mu^-$ (green medium dashed line), combinatorial background (blue medium dashed line), $B_{(s)}^0 \rightarrow h^+h'^-$ (magenta dotted line), $B^{0(+)} \rightarrow \pi^{0(+)}\mu^+\mu^-$ (light blue dot-dashed line), $B^0 \rightarrow \pi^-\mu^+\nu_\mu$ and $B_s^0 \rightarrow K^-\mu^+\nu_\mu$ (black dot-dashed line).

with a significance of 4.0 standard deviations (σ), while the significance of the $B^0 \rightarrow \mu^+\mu^-$ signal is 2.0σ . These significances are determined from the change in likelihood from fits with and without the signal component. The median significance expected for a SM $B_s^0 \rightarrow \mu^+\mu^-$ signal is 5.0σ .

The simultaneous unbinned maximum-likelihood fit results in

$$\begin{aligned} \mathcal{B}(B_s^0 \rightarrow \mu^+\mu^-) &= (2.9_{-1.0}^{+1.1}(\text{stat})_{-0.1}^{+0.3}(\text{syst})) \times 10^{-9}, \\ \mathcal{B}(B^0 \rightarrow \mu^+\mu^-) &= (3.7_{-2.1}^{+2.4}(\text{stat})_{-0.4}^{+0.6}(\text{syst})) \times 10^{-10}. \end{aligned}$$

The statistical uncertainty is derived by repeating the fit after fixing all the fit parameters, except the $B_s^0 \rightarrow \mu^+\mu^-$ and $B^0 \rightarrow \mu^+\mu^-$ branching fractions and the slope and normalisation of the combinatorial background, to their expected values. The systematic uncertainty is obtained by subtracting in quadrature the statistical uncertainty from the total uncertainty obtained from the likelihood with all nuisance parameters allowed to vary according to their uncertainties. Additional systematic uncertainties reflect the impact on the result of changes in the parametrisation of the background by including the $\Lambda_b^0 \rightarrow p\mu^-\bar{\nu}_\mu$ component and by varying the mass shapes of backgrounds from b -hadron decays, and are added in quadrature. The

correlation between the branching fractions parameters of both decay modes is $+3.3\%$. The values of the $B_{(s)}^0 \rightarrow \mu^+\mu^-$ branching fractions obtained from the fit are in agreement with the SM expectations. The invariant mass distribution of the $B_{(s)}^0 \rightarrow \mu^+\mu^-$ candidates with $\text{BDT} > 0.7$ is shown in Fig. 2.

As no significant excess of $B^0 \rightarrow \mu^+\mu^-$ events is found, a modified frequentist approach, the CL_s method [38] is used, to set an upper limit on the branching fraction. The method provides CL_{s+b} , a measure of the compatibility of the observed distribution with the signal plus background hypothesis, CL_b , a measure of the compatibility with the background-only hypothesis, and $\text{CL}_s = \text{CL}_{s+b}/\text{CL}_b$. A search region is defined around the B^0 invariant mass as $m_{B^0} \pm 60 \text{ MeV}/c^2$. For each BDT bin the invariant mass signal region is divided into nine bins with boundaries $m_{B^0} \pm 18, 30, 36, 48, 60 \text{ MeV}/c^2$, leading to a total of 72 search bins.

An exponential function is fitted, in each BDT bin, to the invariant mass sidebands. Even though they do not contribute to the signal search window, the b -hadron backgrounds are added as components in the fit to account for their effect on the combinatorial background estimate. The uncertainty on the expected number of combinatorial background events per bin is determined by applying a Poissonian fluctuation to the number of events observed in the sidebands and by varying the exponential slopes according to their uncertainties. In each bin, the expectations for $B_s^0 \rightarrow \mu^+\mu^-$ decays assuming the SM branching fraction and for $B_{(s)}^0 \rightarrow h^+h'^-$ background are accounted for. For each branching fraction hypothesis, the expected number of signal events is estimated from the normalisation factor. Signal events are distributed in bins according to the invariant mass and BDT calibrations.

In each bin, the expected numbers of signal and background events are computed and compared to the number of observed candidates using CL_s . The expected and observed upper limits for the $B^0 \rightarrow \mu^+\mu^-$

Table 2: Expected limits for the background only (bkg) and background plus SM signal (bkg+SM) hypotheses, and observed limits on the $B^0 \rightarrow \mu^+\mu^-$ branching fraction.

	90 % CL	95 % CL
Exp. bkg	3.5×10^{-10}	4.4×10^{-10}
Exp. bkg+SM	4.5×10^{-10}	5.4×10^{-10}
Observed	6.3×10^{-10}	7.4×10^{-10}

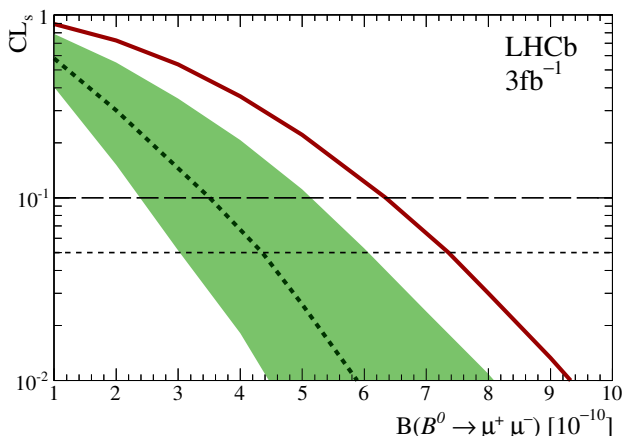


Figure 3: CL_s as a function of the assumed $B^0 \rightarrow \mu^+\mu^-$ branching fraction. The dashed curve is the median of the expected CL_s distribution for background-only hypothesis. The green area covers, for each branching fraction value, 34.1 % of the expected CL_s distribution on each side of its median. The solid red curve is the observed CL_s .

channel are summarised in Table 2 and the expected and observed CL_s values as functions of the branching fraction are shown in Fig. 3.

In summary, a search for the rare decays $B_s^0 \rightarrow \mu^+\mu^-$ and $B^0 \rightarrow \mu^+\mu^-$ is performed with pp collision data corresponding to integrated luminosities of 1 fb^{-1} and 2 fb^{-1} collected at $\sqrt{s} = 7\text{ TeV}$ and 8 TeV , respectively. The B^0 decay yield is not significant and an improved upper limit of $\mathcal{B}(B^0 \rightarrow \mu^+\mu^-) < 7.4 \times 10^{-10}$ at 95 % CL is obtained. The $B_s^0 \rightarrow \mu^+\mu^-$ signal is seen with a significance of 4.0σ . The time-integrated branching fraction $\mathcal{B}(B_s^0 \rightarrow \mu^+\mu^-)$ is measured to be $(2.9_{-1.0}^{+1.1}) \times 10^{-9}$, in agreement with the SM prediction. These measurements supersede and improve on our previous results, and tighten the constraints on possible new physics contributions to these decays.

Acknowledgements

We express our gratitude to our colleagues in the CERN accelerator departments for the excellent performance of the LHC. We thank the technical and administrative staff at the LHCb institutes. We acknowledge support from CERN and from the national agencies: CAPES, CNPq, FAPERJ and FINEP (Brazil); NSFC (China); CNRS/IN2P3 and Region Auvergne (France); BMBF, DFG, HGF and MPG (Germany); SFI (Ireland); INFN (Italy); FOM and NWO (The Netherlands); SCSR (Poland); MEN/IFA (Romania);

MinES, Rosatom, RFBR and NRC “Kurchatov Institute” (Russia); MinECo, XuntaGal and GENCAT (Spain); SNSF and SER (Switzerland); NAS Ukraine (Ukraine); STFC (United Kingdom); NSF (USA). We also acknowledge the support received from the ERC under FP7. The Tier1 computing centres are supported by IN2P3 (France), KIT and BMBF (Germany), INFN (Italy), NWO and SURF (The Netherlands), PIC (Spain), GridPP (United Kingdom). We are thankful for the computing resources put at our disposal by Yandex LLC (Russia), as well as to the communities behind the multiple open source software packages that we depend on.

References

- [1] A. J. Buras, J. Girrbach, D. Guadagnoli, and G. Isidori, *On the Standard Model prediction for $\mathcal{B}(B_{s,d} \rightarrow \mu^+\mu^-)$* , Eur. Phys. J. **C72** (2012) 2172, [arXiv:1208.0934](#).
- [2] A. J. Buras, R. Fleischer, J. Girrbach, and R. Knegjens, *Probing new physics with the $B_s \rightarrow \mu^+\mu^-$ time-dependent rate*, [arXiv:1303.3820](#).
- [3] Heavy Flavor Averaging Group, Y. Amhis *et al.*, *Averages of b-hadron, c-hadron, and τ -lepton properties as of early 2012*, [arXiv:1207.1158](#), updated results and plots available at <http://www.slac.stanford.edu/xorg/hfag/>.
- [4] Fermilab Lattice and MILC collaborations, A. Bazavov *et al.*, *B- and D-meson decay constants from three-flavor lattice QCD*, Phys. Rev. **D85** (2012) 114506, [arXiv:1112.3051](#).
- [5] C. McNeile *et al.*, *High-precision f_{B_s} and heavy quark effective theory from relativistic lattice QCD*, Phys. Rev. **D85** (2012) 031503, [arXiv:1110.4510](#).
- [6] H. Na *et al.*, *B and B_s meson decay constants from lattice QCD*, Phys. Rev. **D86** (2012) 034506, [arXiv:1202.4914](#).
- [7] J. Laiho, E. Lunghi, and R. S. Van de Water, *Lattice QCD inputs to the CKM unitarity triangle analysis*, Phys. Rev. **D81** (2010) 034503, [arXiv:0910.2928](#), updated results available at <http://www.latticeaverages.org/>.
- [8] K. de Bruyn *et al.*, *Probing new physics via the $B_s^0 \rightarrow \mu^+\mu^-$ effective lifetime*, Phys. Rev. Lett. **109** (2012) 041801, [arXiv:1204.1737](#).

- [9] CLEO collaboration, R. Giles *et al.*, *Two-body decays of B mesons*, Phys. Rev. **D30** (1984) 2279.
- [10] CMS collaboration, S. Chatrchyan *et al.*, *Search for $B_s^0 \rightarrow \mu^+\mu^-$ and $B^0 \rightarrow \mu^+\mu^-$ decays*, JHEP **04** (2012) 033, [arXiv:1203.3976](#).
- [11] ATLAS collaboration, G. Aad *et al.*, *Search for the decay $B_s^0 \rightarrow \mu^+\mu^-$ with the ATLAS detector*, Phys. Lett. **B713** (2012) 387, [arXiv:1204.0735](#).
- [12] LHCb collaboration, R. Aaij *et al.*, *First evidence for the decay $B_s^0 \rightarrow \mu^+\mu^-$* , Phys. Rev. Lett. **110** (2013) 021801, [arXiv:1211.2674](#).
- [13] D0 Collaboration, V. M. Abazov *et al.*, *Search for the rare decay $B_s^0 \rightarrow \mu^+\mu^-$* , Phys. Rev. D **87** (2013) 072006, [arXiv:1301.4507](#).
- [14] CDF collaboration, T. Aaltonen *et al.*, *Search for $B_s \rightarrow \mu^+\mu^-$ and $B_d \rightarrow \mu^+\mu^-$ decays with the full CDF Run II data set*, Phys. Rev. **D87** (2013) 072003, [arXiv:1301.7048](#).
- [15] L. Breiman, J. H. Friedman, R. A. Olshen, and C. J. Stone, *Classification and regression trees*, Wadsworth international group, Belmont, California, USA, 1984.
- [16] R. E. Schapire and Y. Freund, *A decision-theoretic generalization of on-line learning and an application to boosting*, Jour. Comp. and Syst. Sc. **55** (1997) 119.
- [17] LHCb collaboration, A. A. Alves Jr. *et al.*, *The LHCb detector at the LHC*, JINST **3** (2008) S08005.
- [18] T. Sjöstrand, S. Mrenna, and P. Skands, *PYTHIA 6.4 physics and manual*, JHEP **05** (2006) 026, [arXiv:hep-ph/0603175](#).
- [19] D. J. Lange, *The EvtGen particle decay simulation package*, Nucl. Instrum. Meth. **A462** (2001) 152.
- [20] Geant4 collaboration, J. Allison *et al.*, *Geant4 developments and applications*, IEEE Trans. Nucl. Sci. **53** (2006) 270; Geant4 collaboration, S. Agostinelli *et al.*, *Geant4: a simulation toolkit*, Nucl. Instrum. Meth. **A506** (2003) 250.
- [21] P. Golonka and Z. Was, *PHOTOS Monte Carlo: a precision tool for QED corrections in Z and W decays*, Eur. Phys. J. **C45** (2006) 97, [arXiv:hep-ph/0506026](#).
- [22] I. Belyaev *et al.*, *Handling of the generation of primary events in GAUSS, the LHCb simulation framework*, Nuclear Science Symposium Conference Record (NSS/MIC) **IEEE** (2010) 1155.
- [23] M. Clemencic *et al.*, *The LHCb simulation application, GAUSS: design, evolution and experience*, J. of Phys: Conf. Ser. **331** (2011) 032023.
- [24] R. Aaij *et al.*, *The LHCb trigger and its performance in 2011*, JINST **8** (2013) P04022, [arXiv:1211.3055](#).
- [25] F. Archilli *et al.*, *Performance of the muon identification at LHCb*, [arXiv:1306.0249](#), submitted to JINST.
- [26] LHCb collaboration, R. Aaij *et al.*, *Strong constraints on the rare decays $B_s^0 \rightarrow \mu^+\mu^-$ and $B^0 \rightarrow \mu^+\mu^-$* , Phys. Rev. Lett. **108** (2012) 231801, [arXiv:1203.4493](#).
- [27] CDF collaboration, A. Abulencia *et al.*, *Search for $B_s^0 \rightarrow \mu^+\mu^-$ and $B_d^0 \rightarrow \mu^+\mu^-$ decays in $p\bar{p}$ collisions with CDF II*, Phys. Rev. Lett. **95** (2005) 221805, [arXiv:hep-ex/0508036](#).
- [28] T. Skwarnicki, *A study of the radiative cascade transitions between the Upsilon-prime and Upsilon resonances*, PhD thesis, Institute of Nuclear Physics, Krakow, 1986, DESY-F31-86-02.
- [29] LHCb collaboration, R. Aaij *et al.*, *Measurement of the fragmentation fraction ratio f_s/f_d and its dependence on B meson kinematics*, JHEP **04** (2013) 1, [arXiv:1301.5286](#).
- [30] LHCb collaboration, *Average f_s/f_d b-hadron production fraction ratio for 7 TeV pp collisions*, LHCb-CONF-2013-011.
- [31] Particle Data Group, J. Beringer *et al.*, *Review of particle physics*, Phys. Rev. **D86** (2012) 010001.
- [32] Y.-M. Wang, Y.-L. Shen, and C.-D. Lu, *$A_b \rightarrow p$, A transition form factors from QCD light-cone sum rules*, Phys. Rev. **D80** (2009) 074012, [arXiv:0907.4008](#).
- [33] W.-F. Wang and Z.-J. Xiao, *Semileptonic decays $B/B_s \rightarrow (\pi, K)(\ell^+\ell^-, \ell\nu, \nu\bar{\nu})$ in the perturbative QCD approach beyond the leading-order*, Phys. Rev. **D86** (2012) 114025, [arXiv:1207.0265](#).
- [34] CDF collaboration, F. Abe *et al.*, *Observation of the B_c meson in $p\bar{p}$ collisions at $\sqrt{s} =$*

- 1.8 TeV , Phys. Rev. Lett. **81** (1998) 2432, [arXiv:hep-ex/9805034](#).
- [35] LHCb collaboration, R. Aaij *et al.*, *First observation of the decay $B^+ \rightarrow \pi^+ \mu^+ \mu^-$* , JHEP **12** (2012) 125, [arXiv:1210.2645](#).
- [36] D. Melikhov and N. Nikitin, *Rare radiative leptonic decays $B_{(d,s)} \rightarrow \ell^+ \ell^- \gamma$* , Phys. Rev. **D70** (2004) 114028, [arXiv:hep-ph/0410146](#).
- [37] Y. G. Aditya, K. J. Healey, and A. A. Petrov, *Faking $B_s \rightarrow \mu^+ \mu^-$* , Phys. Rev. **D87** (2013) 074028, [arXiv:1212.4166](#).
- [38] A. L. Read, *Presentation of search results: the CL_s technique*, J. Phys. **G28** (2002) 2693.